A High Order Semi-implicit Scheme for Ideal Magnetohydrodynamics

Claudius Birke, Walter Boscheri, and Christian Klingenberg

Abstract In this work we design a novel semi-implicit finite volume solver for the equations of ideal magnetohydrodynamics (MHD). The nonlinear convective terms as well as the time evolution of the magnetic field are discretized explicitly, while the terms related to the hydrodynamic pressure in the momentum and in the energy equation are solved implicitly, hence making the scheme particularly well suited for the simulation of low Mach number flows. An elliptic equation is then obtained for the pressure, and the associated system is linearized in time relying on a semi-implicit discretization of the kinetic energy and the enthalpy. High order of accuracy in time is achieved using implicit-explicit Runge-Kutta (IMEX-RK) methods, whereas an efficient CWENO reconstruction permits to gain high accuracy also in space. The solenoidal property of the magnetic field is respected at the discrete level relying on a high order constrained transport method, leading to a structure preserving scheme. The new scheme is conservative for mass, momentum and total energy, and both finite volume and central finite difference discretizations are adopted for the explicit and the implicit terms, respectively, hence introducing no numerical dissipation in the terms related to the pressure. We validate the new schemes against benchmarks for ideal MHD, showing the accuracy and the robustness of the novel methods even in the case of shock waves.

Keywords Semi-implicit · Divergence-free · Compressible low mach number flows · Finite volume schemes · Pressure-based method

W. Boscheri (✉)
Department of Mathematics and Computer Science, University of Ferrara, Ferrara, Italy
e-mail: walter.boscheri@unife.it

C. Birke · C. Klingenberg
Department of Mathematics, University of Würzburg, Würzburg, Germany

E. Franck et al. (eds.), *Finite Volumes for Complex Applications X—Volume 1, Elliptic and Parabolic Problems*, Springer Proceedings in Mathematics & Statistics 432,
https://doi.org/10.1007/978-3-031-40864-9_2

1 Introduction

Magnetized plasma flows are governed by the equations of magnetohydrodynamics (MHD), that describe the time evolution of electric conducting fluids embedded in a magnetic field. The simplest model is given by ideal MHD, where the fluid viscosity is neglected, which constitutes a system of nonlinear hyperbolic partial differential equations (PDE) involving conservation of mass, momentum and total energy coupled with Faraday law for the magnetic field.

The sonic Mach number, which is the ratio between the fluid velocity and the sound speed, describes the regime of the fluid under consideration. The low Mach regime typically arises in astrophysical phenomena such as the generation of magnetic fields in deep convective layers of stars. From the numerical viewpoint, compressible flows are typically discretized using explicit Godunov-type finite volume schemes since they are by construction conservative and thus allow the correct computation of shock waves. However, in the low Mach limit, the effect of numerical viscosity which is added to the numerical fluxes is proven to degrade the accuracy [2, 16]. Furthermore, in the incompressible regime the elliptic behavior of the pressure introduces a very severe restriction on the maximum admissible time step for low Mach number flows, making explicit schemes very ineffective. A possible remedy would be the adoption of fully implicit methods, which inevitably imply the solution of large nonlinear systems that are computationally very expensive and in which the convergence is numerically very difficult to control. Consequently, the MHD system in the low Mach limit has been widely investigated [13, 15, 17, 19, 20, 22, 26]. A successful idea consists in treating implicitly only one part of the system to be solved while keeping the remaining explicit. In this way, the implicit part is relatively simple to be inverted, whereas the nonlinear terms undergo an explicit discretization, making the resulting method capable of dealing with all Mach regimes. This idea has been originally conceived in the context of shallow water and incompressible flows [11, 12], where a semi-implicit time stepping technique has been used. Implicit-explicit (IMEX) schemes have been designed [1, 4–6, 23, 24] in order to deal with multi-scale phenomena, that are typically encountered in compressible fluids.

In this work we propose a novel pressure-based scheme for the solution of the ideal MHD equations. The time discretization is inspired by the class of semi-implicit IMEX schemes [3, 9], and here we treat implicitly the terms related to the pressure, hence not introducing any numerical dissipation and making the CFL stability condition independent from the acoustic wave speed. Differently from [17, 18], no nonlinear equations are used in our approach. Furthermore, the semi-implicit linearization is also used for the kinetic energy, contrarily to what has been proposed in [13].

2 Governing Equations

Let us consider a one-dimensional computational domain $\Omega \in \mathbb{R}$ defined by the spatial coordinate $x \in \Omega$, and let the time coordinate be denoted with $t \in \mathbb{R}_0^+$. The ideal equations of magnetohydrodynamics (MHD) in one space dimension constitute a hyperbolic system of the form

$$\frac{\partial \mathbf{q}}{\partial t} + \frac{\partial \mathbf{f}}{\partial x} = \mathbf{0}, \tag{1}$$

with the vector of state variables $\mathbf{q}$ and the fluxes $\mathbf{f}(\mathbf{q})$ that explicitly write

$$\mathbf{q} = \begin{pmatrix} \rho \\ \rho u \\ \rho v \\ \rho w \\ \rho E \\ B_x \\ B_y \\ B_z \end{pmatrix}, \qquad \mathbf{f}(\mathbf{q}) = \begin{pmatrix} \rho u \\ \rho u^2 + p + \frac{1}{8\pi}\mathbf{B}^2 - \frac{1}{4\pi}B_x^2 \\ \rho uv - \frac{1}{4\pi}B_x B_y \\ \rho uw - \frac{1}{4\pi}B_x B_z \\ u(\rho E + p + \frac{1}{8\pi}\mathbf{B}^2) - \frac{1}{4\pi}B_x(\mathbf{v}\cdot\mathbf{B}) \\ 0 \\ uB_y - vB_x \\ uB_z - wB_x \end{pmatrix}. \tag{2}$$

The fluid density and pressure are addressed with ρ and p, respectively, while $\mathbf{v} = (u, v, w)$ is the velocity field and the magnetic field is denoted with $\mathbf{B} = (B_x, B_y, B_z)$. The total energy ρE is obtained as the sum of three contributions, namely

$$\rho E = \rho e + \rho k + m, \qquad \rho e = \frac{p}{\gamma - 1}, \quad \rho k = \frac{1}{2}\rho \mathbf{v}^2, \quad m = \frac{1}{8\pi}\mathbf{B}^2, \tag{3}$$

where ρk is the kinetic energy and m is the magnetic energy. The internal energy ρe is computed relying on the ideal gas equation of state (EOS) with $\gamma = c_p/c_v$ denoting the ratio of specific heats at constant pressure and volume, respectively. By introducing the specific enthalpy $h = e + p/\rho$, one can reformulate the first part of the energy flux in (2) such that

$$u(\rho E + p + m) = u(\rho k + m) + h(\rho u). \tag{4}$$

The MHD system (2) is hyperbolic since the eigenvalues $\lambda_{i=\{1,\dots,8\}}^{MHD}$ of the associated Jacobian matrix $\mathbf{A} = \partial \mathbf{f}/\partial \mathbf{q}$ with $B_x = const$ are

$$\lambda_{1,8}^{MHD} = u \pm c_f, \quad \lambda_{2,7}^{MHD} = u \pm c_a, \quad \lambda_{3,6}^{MHD} = u \pm c_s, \quad \lambda_4^{MHD} = u, \quad \lambda_5^{MHD} = 0, \tag{5}$$

with the wave speeds given by

$$
\begin{aligned}
c_a &= \frac{B_x}{\sqrt{4\pi\rho}}, \\
c_s^2 &= \frac{1}{2}\left(b^2 + c^2 - \sqrt{(b+c)^2 - 4c_a^2 c^2}\right), \\
c_f^2 &= \frac{1}{2}\left(b^2 + c^2 + \sqrt{(b+c)^2 - 4c_a^2 c^2}\right).
\end{aligned} \tag{6}
$$

The Alfvén wave speed is c_a, the speeds of slow and fast magnetosonic waves are c_s and c_f, respectively, while $c^2 = \gamma p/\rho$ is the adiabatic sound speed that is computed from the ideal equation of state. Furthermore, we use the abbreviation $b^2 = \mathbf{B}^2/(4\pi\rho)$.

The hydrodynamic behavior of the fluid can be analyzed by considering the Mach number $M = u/c$. In the low Mach number limit, the sound speed becomes very high compared to the fluid velocity, hence the terms related to the pressure are dominant. Consequently, larger values of the fast and slow magnetosonic wave speeds are retrieved, and fully explicit numerical methods suffer from both an excessive amount of numerical viscosity, which is proportional to the eigenvalues, and a drastic reduction of the admissible time step Δt to ensure stability under a classical CFL condition of the type

$$
\Delta t \leq \mathrm{CFL} \min_{\Omega} \frac{\max |\lambda^{MHD}|}{\Delta x}, \tag{7}
$$

with Δx denoting the characteristic mesh spacing and the CFL ≤ 1 being the CFL number. Therefore, we propose to discretize implicitly the pressure gradient in the momentum equation and the enthalpy term in the energy equation, while keeping an explicit discretization for the nonlinear convective fluxes and the terms related to the magnetic field. To that aim, let the fluxes be split into a convective-type flux $\mathbf{f}^c(\mathbf{q})$ and a pressure-type flux $\mathbf{f}^p(\mathbf{q})$, that is

$$
\mathbf{f}^c(\mathbf{q}) = \begin{pmatrix}
\rho u \\
\rho u^2 + m - \frac{1}{4\pi} B_x^2 \\
\rho uv - \frac{1}{4\pi} B_x B_y \\
\rho uw - \frac{1}{4\pi} B_x B_z \\
u(\rho k + m) - \frac{1}{4\pi} B_x (\mathbf{v}\cdot\mathbf{B}) \\
0 \\
u B_y - v B_x \\
u B_z - w B_x
\end{pmatrix}, \qquad
\mathbf{f}^p(\mathbf{q}) = \begin{pmatrix}
0 \\ p \\ 0 \\ 0 \\ h\rho u \\ 0 \\ 0 \\ 0
\end{pmatrix}. \tag{8}
$$

We obtain two sub-systems with the following eigenvalues [17].

- Convective sub-system:

$$\frac{\partial \mathbf{q}}{\partial t} + \frac{\partial \mathbf{f}^c}{\partial x} = \mathbf{0}, \tag{9a}$$

$$\lambda^c_{1,8} = u \pm \sqrt{\frac{\mathbf{B}^2}{4\pi\rho}}, \quad \lambda^c_{2,7} = u \pm \frac{B_x}{\sqrt{4\pi\rho}}, \quad \lambda^c_{3,4,5,6} = 0. \tag{9b}$$

- Pressure sub-system:

$$\frac{\partial \mathbf{q}}{\partial t} + \frac{\partial \mathbf{f}^p}{\partial x} = \mathbf{0}, \tag{10a}$$

$$\lambda^p_1 = \frac{1}{2}\left(u - \sqrt{u^2 + 4c^2}\right), \quad \lambda^p_{2,3,4,5,6,7} = 0, \quad \lambda^p_8 = \frac{1}{2}\left(u + \sqrt{u^2 + 4c^2}\right). \tag{10b}$$

It is clear that, by taking the pressure sub-system implicitly, the maximum admissible time step of the scheme becomes

$$\Delta t \leq \mathrm{CFL} \min_{\Omega} \frac{\max |\lambda^c|}{\Delta x}, \tag{11}$$

hence making the scheme particularly well suited for low Mach number flows ($M \ll 1$) where the pressure terms are dominant. On the other hand, for strongly convected flows with shocks, the convective eigenvalues lead the computation of the time step granting stability.

3 Numerical Method

The computational domain $\Omega = [x_L; x_R]$ is discretized using a total number of N_x equidistant cells of volume $\Delta x = (x_R - x_L)/N_x$. The cell centers are indicated with x_i and the cell interfaces are referred to with $x_{i+1/2}$. The time coordinate is bounded in the interval $t \in [0; t_f]$, and the final time t_f is reached performing a sequence of time steps $\Delta t = t^{n+1} - t^n$ that are computed according to the CFL stability condition (11).

3.1 First Order Semi-discrete Scheme in Time

Using the flux splitting (8), it is possible to design the following semi-discrete scheme for the explicit sub-system:

$$\rho^* = \rho^n - \Delta t \frac{\partial}{\partial x} (\rho u)^n , \tag{12a}$$

$$(\rho u)^* = (\rho u)^n - \Delta t \frac{\partial}{\partial x} \left(\rho u^2 + m - \frac{1}{4\pi} B_x^2 \right)^n , \tag{12b}$$

$$(\rho v)^* = (\rho v)^n - \Delta t \frac{\partial}{\partial x} \left(\rho uv - \frac{1}{4\pi} B_x B_y \right)^n , \tag{12c}$$

$$(\rho w)^* = (\rho w)^n - \Delta t \frac{\partial}{\partial x} \left(\rho uw - \frac{1}{4\pi} B_x B_z \right)^n , \tag{12d}$$

$$(\rho E)^* = (\rho E)^n - \Delta t \frac{\partial}{\partial x} \left(u(\rho k + m) - \frac{1}{4\pi} B_x (\mathbf{v} \cdot \mathbf{B}) \right)^n , \tag{12e}$$

$$B_x^* = 0, \tag{12f}$$

$$B_y^* = B_y^n - \Delta t \frac{\partial}{\partial x} \left(u B_y - v B_x \right)^n , \tag{12g}$$

$$B_z^* = B_z^n - \Delta t \frac{\partial}{\partial x} (u B_z - w B_x)^n . \tag{12h}$$

The above definitions are then employed to obtain a first order semi-implicit time discretization [3, 9, 10] of the MHD equations (2), which writes

$$\rho^{n+1} = \rho^*, \tag{13a}$$

$$(\rho u)^{n+1} = (\rho u)^* - \Delta t \frac{\partial}{\partial x} \left(p^{n+1} \right), \tag{13b}$$

$$(\rho v)^{n+1} = (\rho v)^*, \tag{13c}$$

$$(\rho w)^{n+1} = (\rho w)^*, \tag{13d}$$

$$(\rho e)^{n+1} + \frac{(\rho u)^{n+1} (\rho u)^n}{2\rho^{n+1}} + m^{n+1} = (\rho E)^* - \Delta t \frac{\partial}{\partial x} \left(h^n (\rho u)^{n+1} \right), \tag{13e}$$

$$B_x^{n+1} = B_x^*, \tag{13f}$$

$$B_y^{n+1} = B_y^*, \tag{13g}$$

$$B_z^{n+1} = B_z^*. \tag{13h}$$

To avoid nonlinear implicit terms, let us notice that the implicit flux in the energy equation has been discretized by taking the enthalpy explicitly, and the kinetic energy in the total energy definition splits into an explicit and an implicit contribution:

$$(\rho E)^{n+1} := (\rho e)^{n+1} + \frac{(\rho u)^{n+1} (\rho u)^n}{2\rho^{n+1}} + m^{n+1}, \tag{14}$$

following the approach presented in [9] for the hydrodynamics equations. Recall that the internal energy can be expressed in terms of the pressure relying on the ideal gas EOS (3), and that the new magnetic energy $m^{n+1} = (\mathbf{B}^{n+1})^2/(8\pi)$ can be explicitly computed because the fluxes of the magnetic field belong to the explicit sub-system

(9). Moreover, the time evolution of the density is also concerned with an explicit update, hence making ρ^{n+1} already known from (12a). Therefore, a preliminary discretization of the total energy equation is chosen by inserting the momentum equation (13b) into the energy equation (13e) leading to an elliptic equation for the pressure:

$$\frac{p^{n+1}}{\gamma-1}-\Delta t\frac{(\rho u)^n}{2\rho^{n+1}}\frac{\partial}{\partial x}\left(p^{n+1}\right)-\Delta t^2\frac{\partial}{\partial x}\left(h^n\frac{\partial}{\partial x}\left(p^{n+1}\right)\right)=b^n, \tag{15}$$

with the known right-hand-side given by

$$b^n=(\rho E)^*-\frac{(\rho u)^n}{2\rho^{n+1}}(\rho u)^*-m^{n+1}-\Delta t\frac{\partial}{\partial x}\left(h^n(\rho u)^*\right). \tag{16}$$

The pressure equation (15) constitutes a linear system for the scalar unknown p^{n+1} that is solved using the iterative GMRES solver [25] up to a prescribed tolerance (we typically set tol $=10^{-12}$). Differently from [17, 18], this approach does not need any fixed point method thanks to the semi-implicit splitting of the enthalpy flux and the kinetic energy in the energy equation. Once the new pressure is known, the new momentum $(\rho u)^{n+1}$ is updated with (13b), and then the new total energy is updated using the conservative formulation

$$(\rho E)^{n+1}=(\rho E)^*-\Delta t\frac{\partial}{\partial x}\left(h^n(\rho u)^{n+1}\right). \tag{17}$$

3.2 First Order Discrete Spatial Operators

The spatial operators are given by both finite volume and finite difference approximations, and they are introduced hereafter referring to the state vector $\mathbf{q}(x,t)$.

The convective sub-system (9) is discretized with a conservative Godunov-type finite volume method, that is

$$\mathbf{q}_i^*=\mathbf{q}_i^n-\frac{\Delta t}{\Delta x}\left(\mathbf{f}^c_{i+1/2}-\mathbf{f}^c_{i-1/2}\right). \tag{18}$$

We choose to use the simple Rusanov-type numerical flux $\mathbf{f}^c_{i+1/2}$ that is given by

$$\mathbf{f}^c_{i+1/2}=\frac{1}{2}\left(\mathbf{f}^c(\mathbf{q}_{i+1})+\mathbf{f}^c(\mathbf{q}_i)\right)-\frac{1}{2}s_{\max}\left(\mathbf{q}_{i+1}-\mathbf{q}_i\right), \tag{19}$$

where the numerical dissipation $s_{\max}=\max\left(|\lambda^c_{i+1}|,|\lambda^c_i|\right)$ only accounts for the convective eigenvalues, thus no acoustic speed is involved.

The implicit terms appearing in the pressure sub-system (10) are approximated by means of finite difference operators with no numerical dissipation, thus one has

$$\left.\frac{\partial \mathbf{q}}{\partial x}\right|_i^{n+1} = \frac{\mathbf{q}_{i+1}^{n+1} - \mathbf{q}_{i-1}^{n+1}}{2\,\Delta x} + O(\Delta x^2), \tag{20a}$$

$$\left.\frac{\partial}{\partial x}\left(h\frac{\partial \mathbf{q}}{\partial x}\right)\right|_i^{n,n+1} = \frac{1}{\Delta x^2}\left[h_{i-1}^n\, h_i^n\, h_{i+1}^n\right]\begin{bmatrix} 3/4 & -1 & 1/4 \\ 0 & 0 & 0 \\ 1/4 & -1 & 3/4 \end{bmatrix}\begin{bmatrix} \mathbf{q}_{i-1}^{n+1} \\ \mathbf{q}_i^{n+1} \\ \mathbf{q}_{i+1}^{n+1} \end{bmatrix} + O(\Delta x^2). \tag{20b}$$

3.3 Extension to High Order of Accuracy

The semi-discrete first order scheme (13) supplemented with the spatial operators (18)–(20) is extended to high order of accuracy in space and time by means of semi-implicit IMEX Runge-Kutta methods [3] and quadrature-free CWENO reconstructions [9], respectively.

High order in time. The governing equations are written under the form of an autonomous system with initial condition $\mathbf{q}(t_0) = \mathbf{q}_0$:

$$\frac{\partial \mathbf{q}}{\partial t} = \mathcal{H}(\mathbf{q}_E(t), \mathbf{q}_I(t)), \tag{21}$$

where the spatial fluxes are contained in the flux term $\mathcal{H}(\mathbf{q}_E(t), \mathbf{q}_I(t))$ according to (8), hence involving both explicit and implicit terms, namely $\mathbf{q}_E(t)$ and $\mathbf{q}_I(t)$, respectively. Implicit-explicit (IMEX) Runge-Kutta schemes [24] are then used to advance the solution in time of system (21), following a method of lines (MOL) philosophy. After having set $\mathbf{q}_E = \mathbf{q}_I = \mathbf{q}^n$, the stage fluxes for $r = 1, \ldots, s$ are computed in the following way:

$$\mathbf{q}_E^r = \mathbf{q}_E^n + \Delta t \sum_{\ell=1}^{r-1} \tilde{a}_{r\ell} k_\ell, \qquad 2 \le r \le s, \tag{22a}$$

$$\tilde{\mathbf{q}}_I^r = \mathbf{q}_E^n + \Delta t \sum_{\ell=1}^{r-1} a_{r\ell} k_\ell, \qquad 2 \le r \le s, \tag{22b}$$

$$k_r = \mathcal{H}\left(\mathbf{q}_E^r, \tilde{\mathbf{q}}_I^r + \Delta t\, a_{rr}\, k_r\right). \qquad 1 \le r \le s. \tag{22c}$$

The coefficients $\tilde{a}_{r\ell}$ and $a_{r\ell}$ refer to the explicit and the implicit Runge-Kutta scheme, respectively, and they are collected in a double Butcher tableau. We employ stiffly accurate schemes [3], therefore the solution at the new time level is simply given by the solution of the last stage of the RK time stepping, that is $\mathbf{q}_E^s = \mathbf{q}_I^s = \mathbf{q}^{n+1}$. The interested reader is referred to [3].

High order in space. To increase the spatial accuracy, the numerical fluxes in the finite volume scheme (18) are fed with high order extrapolated data from the cells sharing the interface. A CWENO reconstruction [21] is performed because it allows for relatively compact stencils even for higher order reconstructions. Specifically, we rely on the very efficient dimension-by-dimension technique forwarded in [9], which ultimately yields a quadrature-free finite volume scheme. By denoting the reconstruction operator with $\mathbb{R}(\mathbf{q})$, the high order numerical fluxes are simply given by

$$\mathbf{f}^c_{i+1/2} = \frac{1}{2}\left(\mathbf{f}^c(\mathbb{R}(\mathbf{q}_{i+1})) + \mathbf{f}^c(\mathbb{R}(\mathbf{q}_i))\right) - \frac{1}{2} s_{\max}\left(\mathbb{R}(\mathbf{q}_{i+1}) - \mathbb{R}(\mathbf{q}_i)\right), \tag{23}$$

where the reconstruction operator must be evaluated at the interface $x_{i+1/2}$. High order finite difference operators are adopted for the implicit terms (20). Further details can be found in [9].

Remark on high Mach number flows. There is no advantage in our method for purely high Mach number flows, where indeed it would be much better to use classical explicit finite volume solvers. To track the shocks, the time step must be still determined taking into account the sound speed according to (7), at the computational price of the solution of the linear system (15). Nevertheless, our numerical scheme is stable even if the time step is chosen larger, namely according to (11), which is not the case for explicit schemes. This might turn to be useful in the case of coexisting different regimes, i.e. low and high Mach number flows, that may occur in the flow at the same time. In this situation, our approach still allows for a rather large time step, which will capture the stiff limit of the model while being stable across shocks.

3.4 Divergence-Free Involution in Multiple Space Dimensions

The extension of the semi-implicit IMEX scheme (13) to multiple space dimensions is carried out considering a Cartesian mesh in both y and z direction, therefore it is straightforward. However, in multiple space dimensions, we must take care of the solenoidal property of the magnetic field, that endows the MHD system with the following involution:

$$\nabla \cdot \mathbf{B} = 0. \tag{24}$$

To respect this condition at the discrete level, we rely on the constrained transport method presented in [14], which corrects the magnetic field by approximating the curl of the magnetic vector potential $\mathbf{A}$ such that $\mathbf{B} = \nabla \times \mathbf{A}$ with a fourth order finite difference scheme. The resulting magnetic field is then proven to be divergence-free by applying a discrete finite difference operator to the discrete curl operator. High order div-curl operators have been recently considered in [7], while curl-free structure

preserving schemes have been designed in [8]. All the details of the divergence-free evolution of the magnetic field are reported in [14].

4 Numerical Results

In all the following numerical test problems, the time step is computed according to (11) with CFL $= 0.9$ and the ratio of specific heats is set to $\gamma = 5/3$. Furthermore, the magnetic field is verified to respect the divergence-free condition (24) up to machine precision by measuring the maximum divergence error over the whole domain using a finite difference approximation. Finally, the permeability of the magnetic field is normalized to unity.

4.1 Numerical Convergence Studies

The numerical convergence study is carried out by considering a smooth MHD vortex problem, according to the setup given in [17]. We run second and third order space-time accurate semi-implicit schemes until the final time $t_f = 1$. The results are reported in Table 1, demonstrating that the formal order of accuracy is achieved.

Furthermore, along the lines of [20], we run this problem for different values of the Mach number, namely we consider a vortex with $M = 1.55 \cdot 10^{-5}$, $M = 1.55 \cdot 10^{-4}$ and $M = 1.55 \cdot 10^{-3}$. From the analysis shown in Table 2, we can conclude that the

Table 1 Numerical convergence results for the ideal MHD equations equations using the semi-implicit finite volume schemes (SIFV) for second and third order of accuracy in space and time. The errors are measured in the L_2 norm and refer to the variable u (velocity component in the $x-$direction), p (pressure) and B_x (magnetic field component in the $x-$direction) at time $t_f = 0.1$

SIFV $O(2)$						
$N_x = N_y$	$L_2(u)$	$O(u)$	$L_2(p)$	$O(p)$	$L_2(B_x)$	$O(B_x)$
24	7.633E-03	–	6.351E-03	–	2.350E-03	–
32	3.801E-03	2.42	3.212E-03	2.37	1.107E-03	2.16
48	1.512E-03	2.27	1.271E-03	2.29	4.191E-04	2.40
64	8.309E-04	2.08	6.821E-04	2.16	2.223E-04	2.20
SIFV $O(3)$						
$N_x = N_y$	$L_2(u)$	$O(u)$	$L_2(p)$	$O(p)$	$L_2(B_x)$	$O(B_x)$
24	5.485E-03	–	5.091E-03	–	1.879E-03	–
32	2.364E-03	2.93	2.397E-03	2.62	7.675E-04	3.11
48	7.228E-04	2.92	8.494E-04	2.56	2.213E-04	3.07
64	3.062E-04	2.99	4.188E-04	2.42	9.620E-05	2.90

Table 2 Numerical convergence results for the ideal MHD equations using the semi-implicit finite volume schemes (SIFV) for third order of accuracy in space and time running the smooth vortex test cases at different Mach numbers. The errors are measured in the L_2 norm and refer to the variable B_x (magnetic field component in the $x-$direction) at time $t_f = 0.1$

	$M = 1.55 \cdot 10^{-5}$		$M = 1.55 \cdot 10^{-4}$		$M = 1.55 \cdot 10^{-3}$	
$N_x = N_y$	$L_2(B_x)$	$O(B_x)$	$L_2(B_x)$	$O(B_x)$	$L_2(B_x)$	$O(B_x)$
24	3.831E-04	–	3.832E-03	–	3.835E-02	–
32	4.461E-05	3.10	4.461E-04	3.10	4.466E-03	3.10
48	5.257E-06	3.08	5.255E-05	3.09	5.259E-04	3.09
64	6.448E-07	3.03	6.438E-06	3.03	4.450E-05	3.03

novel schemes are asymptotic preserving and asymptotic accurate, meaning that no loss of accuracy is observed for low Mach regimes. The distribution of magnetic pressure and hydrodynamics pressure are shown in Fig. 1, where the structure of the vortex is well preserved independently from the Mach number.

4.2 Riemann Problems

In this section, we apply the semi-implicit finite volume scheme to a set of four different Riemann problems of the ideal MHD equations taken from the literature [17, 18]. The aim of this set of test problems is to demonstrate the capability of the semi-implicit scheme to deal with shocks, thus not in the low Mach regime of the fluid. The initial left and right states, which are separated by a discontinuity located at x_d, are listed in Table 3. The computational domain for all Riemann problems is set to $\Omega = [0; 1]$ and the specific heat is defined by $\gamma = 2.0$ for RP1 and $\gamma = \frac{5}{3}$ for the rest. We use a discretization of 200 grid cells for the simulations with the semi-implicit method and the results are compared with those derived by a fully explicit finite volume method using the Rusanov flux on 1024 grid cells. Both methods have second order accuracy in time and space. The comparison between the solution obtained with the semi-implicit scheme and the reference solution is presented in Fig. 2. The results show that the semi-implicit scheme is able to properly capture and resolve the different waves. Only for B_y in RP2 and RP4 the resolution is not sufficient to reproduce every discontinuity in a similar manner as the reference solution. Overall, the results are consistent with those retrieved with other numerical methods in the literature [17, 18].

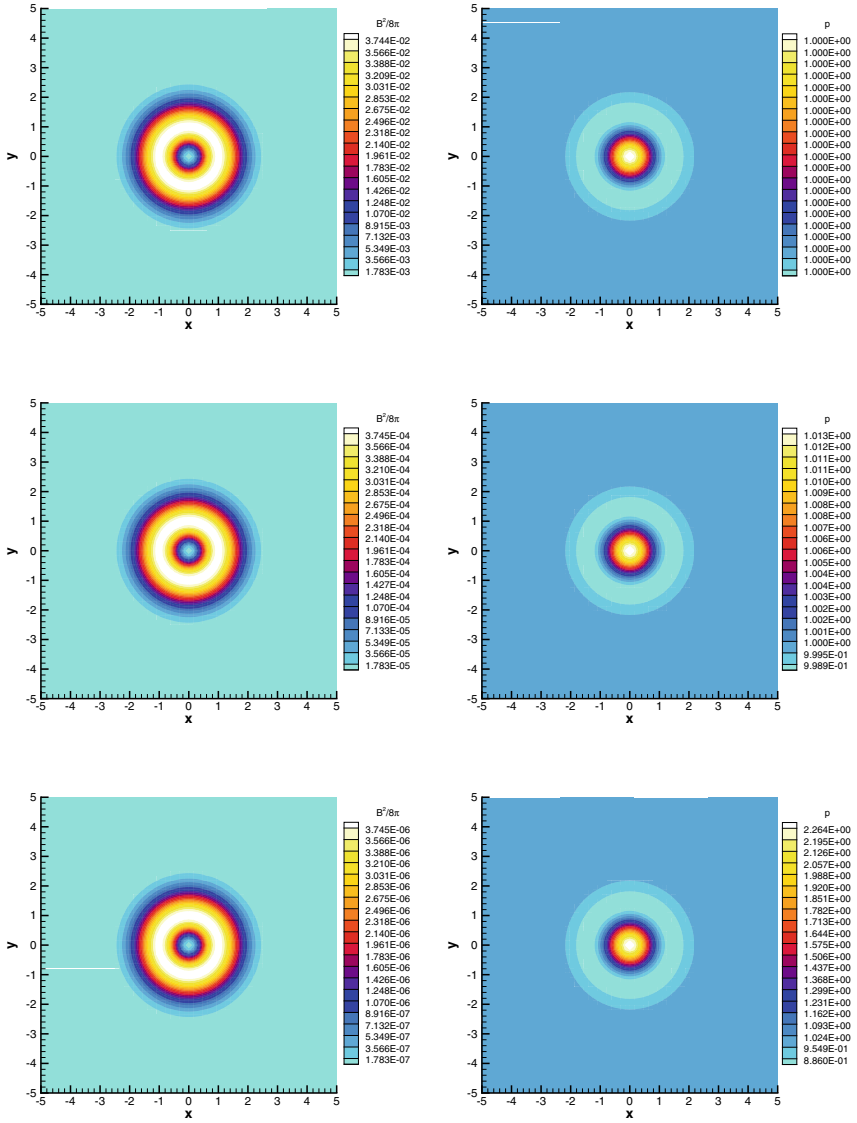

Fig. 1 Smooth MHD vortex. Numerical solution at $t_f = 1$ of magnetic pressure (left column) and hydrodynamics pressure (right column) for Mach number $M = 1.55 \cdot 10^{-3}$ (top), $M = 1.55 \cdot 10^{-4}$ (middle) and $M = 1.55 \cdot 10^{-5}$ (bottom)

Table 3 Initial values for the left and right state for different Riemann problems and the location of the initial discontinuity x_d

Case		x_d	t_f	ρ	u	v	w	p	B_x	B_y	B_z
RP1	L:	0.5	0.12	1.0	0.0	0.0	0.0	1.0	0.75	1.0	0.0
	R:			0.125	0.0	0.0	0.0	0.1	0.75	−1.0	0.0
RP2	L:	0.4	0.2	1.08	1.2	0.01	0.5	0.95	$2.0/\sqrt{4\pi}$	$3.6/\sqrt{4\pi}$	$2.0/\sqrt{4\pi}$
	R:			0.9891	−0.0131	0.0269	0.010037	0.97159	$2.0/\sqrt{4\pi}$	$4.0244/\sqrt{4\pi}$	$2.0026/\sqrt{4\pi}$
RP3	L:	0.4	0.15	1.7	0.0	0.0	0.0	1.7	$3.899398/\sqrt{4\pi}$	$3.544908/\sqrt{4\pi}$	0.0
	R:			0.2	0.0	0.0	−1.496891	0.2	$3.899398/\sqrt{4\pi}$	$2.785898/\sqrt{4\pi}$	$2.192064/\sqrt{4\pi}$
RP4	L:	0.5	0.16	1.0	0.0	0.0	0.0	1.0	1.3	1.0	0.0
	R:			0.4	0.0	0.0	0.0	0.4	1.3	−1.0	0.0

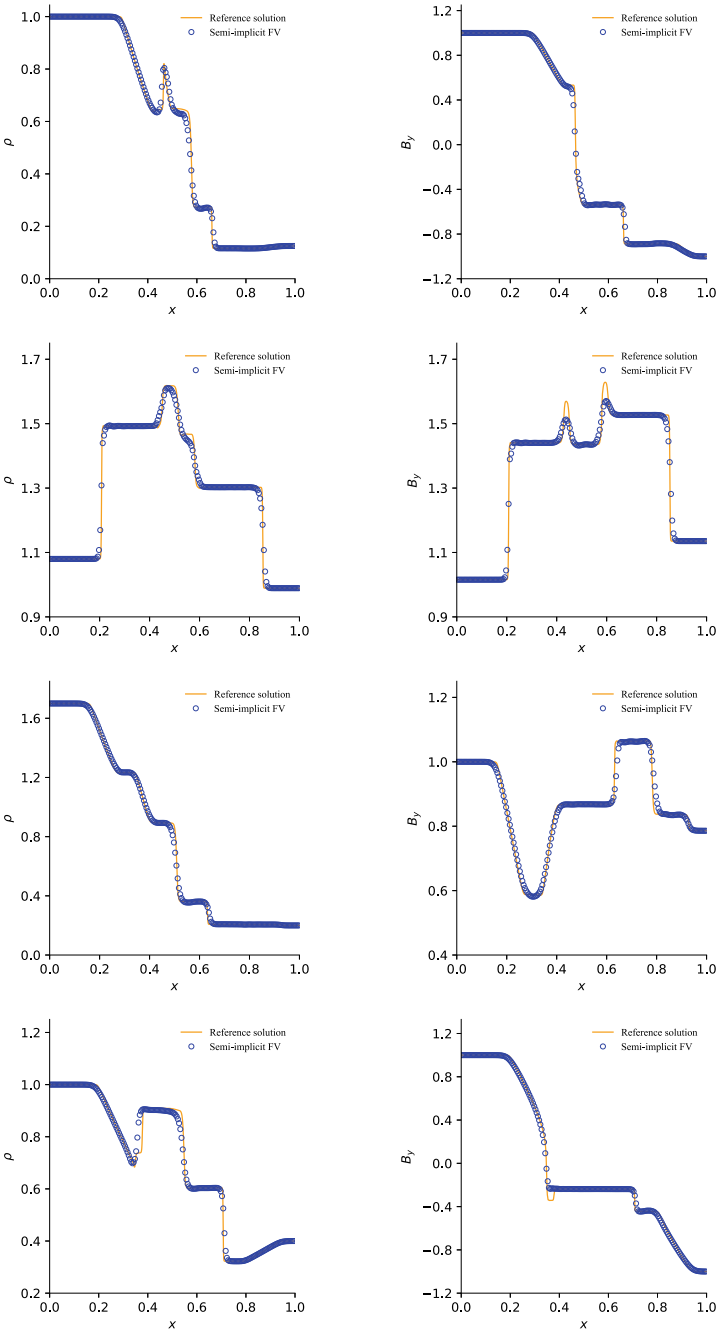

Fig. 2 Riemann problem RP1, RP2, RP3 and RP4 (from top to bottom row) at the final time $t = t_f$. Comparison of density (left column) and magnetic field component B_y (right column) against the reference solution

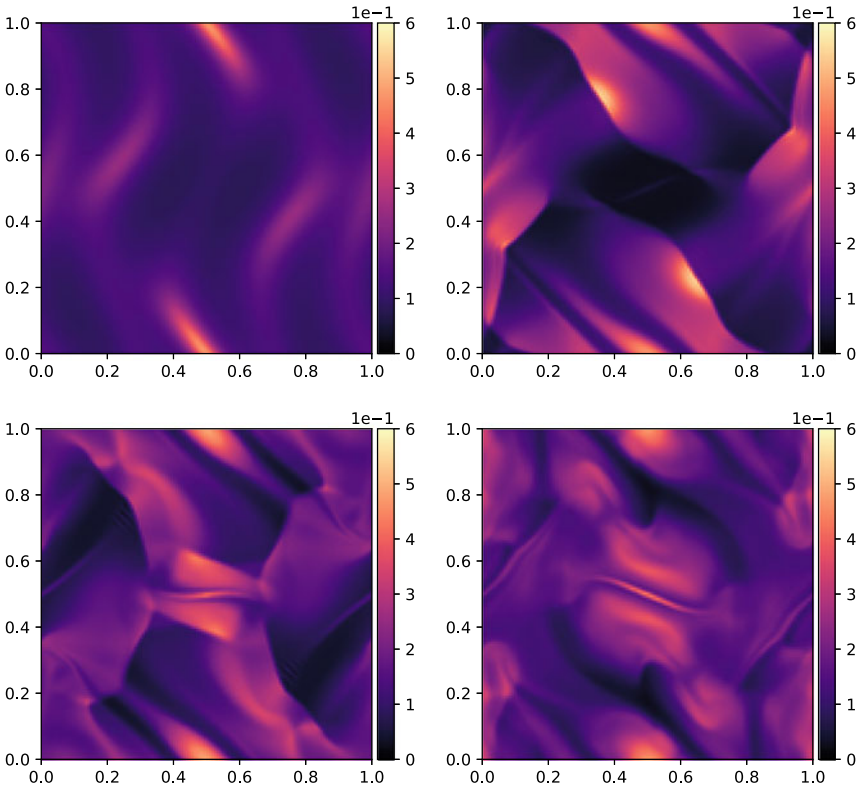

Fig. 3 Orszag-Tang vortex. Numerical solution of pressure at output time $t = 1/12$ (top left), $t = 1/3$ (top right), $t = 0.5$ (bottom left) and $t = 5/6$ (bottom right)

4.3 Orszag-Tang Vortex

A widely used test for the two-dimensional MHD equations is the Orszag Tang vortex [14, 17]. Starting with smooth initial data, over time shocks develop along the diagonal direction in combination with a vortex located at the center of the computational domain. On the spatial domain $\Omega = [0; 1]^2$ the initial condition for the state variables $\mathbf{q}$ is given by

$$\begin{aligned}&\mathbf{q}(0, x, y)\\ &= \left(\frac{25}{36\pi},\ -\sin(2\pi y),\ \sin(2\pi x),\ 0.0,\ \frac{5}{12\pi},\ -\frac{1}{\sqrt{4\pi}}\sin(2\pi y),\ \frac{1}{\sqrt{4\pi}}\sin(4\pi x)\right)\end{aligned} \tag{25}$$

and the magnetic vector potential $\mathbf{A}$ is initially defined by

$$\mathbf{A}(0, x, y) = \left(0.0,\ 0.0,\ \cos(2\pi y)/(4\pi^{3/2}) + \cos(4\pi x)/(8\pi^{3/2})\right). \tag{26}$$

Periodic boundary conditions are imposed on all sides. The computational domain is discretized by a 128×128 control volumes. In Fig. 3 the results for the pressure at different times computed by the third-order semi-implicit method are presented. The numerical method manages to capture the shocks that occur as time evolves. Overall, the results are qualitatively consistent with those in the literature [14, 17].

5 Conclusions

In this work we have presented a pressure-based semi-implicit scheme for the solution of the ideal MHD equations. An elliptic equation for the pressure is obtained to solve low Mach regimes very efficiently without adding any numerical dissipation in the implicit part. On the other hand, an explicit finite volume solver is adopted for handling the nonlinear convective terms, endowing our scheme with shock-capturing properties. The scheme is conservative for mass, momentum and total energy. High order of accuracy is achieved by means of a CWENO reconstruction in space and IMEX Runge-Kutta time stepping techniques. The accuracy and the robustness of the scheme have been demonstrated by performing a numerical convergence study for different Mach numbers and by solving a set of Riemann problems. Another benchmark in numerical MHD has been shown, namely the Orszag-Tang vortex test, proving the capability of the novel method to deal with complex magnetized flows and to provide results which are qualitatively in agreement with other existing numerical schemes in the literature.

Acknowledgements WB received financial support by Fondazione Cariplo and Fondazione CDP (Italy) under the project No. 2022-1895. WB also acknowledges fundings from the Italian Ministry of University and Research (MUR) with the PRIN Project 2022 No. 2022N9BM3N. CB acknowledges the support by the German Research Foundation (DFG) under the project No. KL 566/22-1.

References

1. Ascher, U.M., Ruuth, S.J., Spiteri, R.J.: Implicit-explicit Runge-Kutta methods for time-dependent partial differential equations. Appl. Numer. Math. **25**, 151–167 (1982)
2. Barsukow, W., Edelmann, P., Klingenberg, C., Röpke, F.: A low-Mach Roe-type solver for the Euler equations allowing for gravity source terms. ESAIM: Proc. Surv. **58**, 27–39 (2017)
3. Boscarino, S., Filbet, F., Russo, G.: High order semi-implicit schemes for time dependent partial differential equations. J. Sci. Comput. **68**, 975–1001 (2016)
4. Boscarino, S., Pareschi, L.: On the asymptotic properties of IMEX Runge-Kutta schemes for hyperbolic balance laws. J. Comput. Appl. Math. **316**, 60–73 (2017)
5. Boscarino, S., Pareschi, L., Russo, G.: A unified IMEX Runge-Kutta approach for hyperbolic systems with multiscale relaxation. SIAM J. Numer. Anal. **55**(4), 2085–2109 (2017)
6. Boscarino, S., Russo, G.: On a class of uniformly accurate IMEX Runge-Kutta schemes and applications to hyperbolic systems with relaxation. SIAM J. Sci. Comput. **31**, 1926–1945 (2009)

7. Boscheri, W., Dimarco, G., Pareschi, L.: Locally Structure-Preserving div-curl operators for high order Discontinuous Galerkin schemes. J. Comput. Phys. **486**, 112130 (2023)
8. Boscheri, W., Dumbser, M., Ioriatti, M., Peshkov, I., Romenski, E.: A structure-preserving staggered semi-implicit finite volume scheme for continuum mechanics. J. Comput. Phys. **424**, 109866 (2021)
9. Boscheri, W., Pareschi, L.: High order pressure-based semi-implicit IMEX schemes for the 3D Navier-Stokes equations at all Mach numbers. J. Comput. Phys. **434**, 110206 (2021)
10. Boscheri, Walter, Tavelli, Maurizio: High order semi-implicit schemes for viscous compressible flows in 3d. Appl. Math. Comput. **434**, 127457 (2022)
11. Casulli, V.: Semi-implicit finite difference methods for the two-dimensional shallow water equations. J. Comput. Phys. **86**, 56–74 (1990)
12. Casulli, V.: A semi-implicit finite difference method for non-hydrostatic free-surface flows. Int. J. Num. Meth. Fluids **30**, 425–440 (1999)
13. Chen, W., Wu, K., Xiong, T.: High order asymptotic preserving finite difference weno schemes with constrained transport for MHD equations in all sonic mach numbers. Astron. Astrophys. (2022)
14. Christlieb, Andrew J., Rossmanith, James A., Tang, Qi.: Finite difference weighted essentially non-oscillatory schemes with constrained transport for ideal magnetohydrodynamics. J. Comput. Phys. **268**, 302–325 (2014)
15. Cui, Wenqian, Yaobin, Ou., Ren, Dandan: Incompressible limit of full compressible magnetohydrodynamic equations with well-prepared data in 3-d bounded domains. J. Math. Anal. Appl. **427**(1), 263–288 (2015)
16. Dellacherie, S.: Analysis of Godunov type schemes applied to the compressible Euler system at low Mach number. J. Comput. Phys. **229**, 978–1016 (2010)
17. Dumbser, M., Balsara, D.S., Tavelli, M., Fambri, F.: A divergence-free semi-implicit finite volume scheme for ideal, viscous, and resistive magnetohydrodynamics. Int. J. Numer. Methods Fluids **89**, 16–42 (2019)
18. Fambri, F.: A novel structure preserving semi-implicit finite volume method for viscous and resistive magnetohydrodynamics. Int. J. Numer. Methods Fluids **93**, 3447–3489 (2021)
19. Jiang, S., Ju, Q., Li, F.: Incompressible limit of the compressible magnetohydrodynamic equations with periodic boundary conditions. Commun. Math. Phys. **297**, 371–400 (2010)
20. Leidi, G., Birke, C., Andrassy, R., Higl, J., Edelmann, P.V.F., Wiest, G., Klingenberg, C., Röpke, F.K.: A finite-volume scheme for modeling compressible magnetohydrodynamic flows at low Mach numbers in stellar interiors. Astron. Astrophys. **668**, A143 (2022)
21. Levy, D., Puppo, G., Russo, G.: Central WENO schemes for hyperbolic systems of conservation laws. M2AN Math. Model. Numer. Anal. **33**(3), 547–571 (1999)
22. Mamashita, Tomohiro, Kitamura, Keiichi, Minoshima, Takashi: Slau2-hlld numerical flux with wiggle-sensor for stable low mach magnetohydrodynamics simulations. Comput. Fluids **231**, 105165 (2021)
23. Osher, S., Solomon, F.: A partially implicit method for large stiff systems of Ode's with only few equations introducing small time-constants. SIAM J. Numer. Anal. **13**, 645–663 (1976)
24. Pareschi, L., Russo, G.: Implicit-explicit Runge-Kutta schemes and applications to hyperbolic systems with relaxation. J. Sci. Comput. **25**, 129–155 (2005)
25. Saad, Y., Schultz, M.: GMRES: a generalized minimal residual algorithm for solving nonsymmetric linear systems. SIAM J. Sci. Stat. Comput. **7**, 856–869 (1986)
26. Thomann, A., Puppo, G., Klingenberg, C.: An all speed second order well-balanced IMEX relaxation scheme for the Euler equations with gravity. J. Comput. Phys. **420**, 109723 (2020)